Avrupa Bilim ve Teknoloji Dergisi
Özel Sayı 28, S. 675-683, Kasım 2021
© Telif hakkı EJOSAT'a aittir
**Araştırma Makalesi**

www.ejosat.com ISSN:2148-2683

European Journal of Science and Technology
Special Issue 28, pp. 675-683, November 2021
Copyright © 2021 EJOSAT
**Research Article**

# Impact of $Fe_3O_4$/water on Natural Convection in Square Enclosure

Hayati Kadir Pazarlioglu [1*], Mutlu Tekir [2]

[1*] Karabuk University, Faculty of Engineering, Department of Mechanical Engineering, Karabuk, Turkey, (ORCID: 0000-0002-9365-9431), hayatikadirpazarlioglu@gmail.com

[2] Karabuk University, Faculty of Engineering, Department of Medical Engineering, Karabuk, Turkey, (ORCID: 0000-0003-2289-7034), mutlutekir@karabuk.edu.tr

(1st International Conference on Applied Engineering and Natural Sciences ICAENS 2021, November 1-3, 2021)

(**DOI:** 10.31590/ejosat.1010066)

**ATIF/REFERENCE:** Pazarlioglu, H. K., & Tekir, M. (2021). Impact of Fe3O4/water on Natural Convection in Square Enclosure, (28), 675-683.

**Abstract**

Natural convection characteristics in a 2D square enclosure (10 *mm* x 10 *mm*) have been investigated detailly under natural convection conditions ($10^3 \leq Gr \leq 10^5$). A model has been developed to analyze the dispersed nanoparticle effect on natural convection performance in an enclosure. The left vertical wall is maintained at a high temperature, while the right vertical wall is kept at a low temperature, whereas horizontal walls are assumed to be insulated. $Fe_3O_4$/water ($0 \leq \varphi \leq 1.0$) nanofluid has been utilized to analyze the convection enhancement in the enclosure. To elucidate flow characteristics and heat transfer performance of $Fe_3O_4$/water nanofluid, temperature, velocity streamline, and vorticity contours have been taken place. It is concluded that nanoparticle dispersion in base fluid enhances the natural convection heat transfer. Also, Grashof number has an important role in heat transfer mechanism.

**Keywords:** Natural convection, enclosure, Grashof number, Fe3O4/water, nanofluid, CFD

# Kare Kutu İçinde $Fe_3O_4$/Su'yun Doğal Konveksiyona Etkisi

**Öz**

Doğal konveksiyon altında ($10^3 \leq Gr \leq 10^5$) 2D kutu içindeki (10 *mm* x 10 *mm*) $Fe_3O_4$/water karakteristiği detaylı olarak incelenmiştir. Modelimiz bir kutu içinde doğal konveksiyonun nano akışkanın varlığı durumunda analiz etmek için geliştirilmiştir. Sol duvar sıcak duvar, sağ duvar soğuk sıcaklıkta sabit tutulurken, yatay duvarlar yalıtımlı olarak tutulmuştur. $Fe_3O_4$/water ($0 \leq \varphi \leq 1.0$) nanoakışkanı kutu içindeki konvektif iyileştirmeyi analiz etmek için kullanılmıştır. $Fe_3O_4$/water nanoakışkanının akış karakteristiğimi ve ısı transferi performansı analiz etmek için sıcaklık eş eğrisi, hız akış çizgisi ve girdap akış çizgisi oluşturulmuştur. Sonuç olarak, baz akışkan içine nanoakışkan karıştırılması doğal konveksiyonu iyileştirmektedir. Ayrıca Grashof sayısı ısı transferi mekanizmasında önemli bir role sahiptir.

**Anahtar Kelimeler:** Doğal konveksiyon, kutu, Grashof sayısı, $Fe_3O_4$/su, nanofluid, HAD

* Corresponding Author: xxxx@xxx.xx.xx

# 1. Introduction

Natural convection occurs due to temperature gradient and is mostly encountered as a type of heat transfer mechanism in the industry. Buoyancy-driven natural convection takes place in reactor chambers of nuclear power plants, microelectronics cooling [1], solar air heaters [2], large-scale meteorology [3,4]. Kim et al. [5] investigated the natural convection in a square enclosure numerically using immersed boundary method. The cylinder has been heated in the enclosure and natural convection took place under $10^3 \leq Ra \leq 10^7$ conditions. It is seen that vortex generation in the enclosure and the height of the cylinder are related. Bhattacharya and Basak [6] studied the natural convection in a square enclosure with a non-isothermal hot bottom wall, isothermal sidewalls, and insulated top wall. Under the conditions of $10^2 \leq Ra \leq 10^6$ steady-state numerical analyses have been accomplished, and flow structures have been visualized. It is understood that increasing Rayleigh number *(Ra)* has a greater effect on the convective heat transfer rate. Hadidi et al. [7] investigated the natural convection in an inclined square enclosure. The effects of the thickness of a porous layer, Rayleigh number, buoyancy ratio, Lewis number, cavity inclination angle, and the thermal conductivity ratio on the heat transfer performance have been examined in detail. It is concluded that Rayleigh number, cavity inclination angle, and thermal conductivity have a stronger effect on heat transfer rate in comparison with other parameters used in this study. Also, Liang et al. [8] studied the inclined square enclosure between -90˚ and 90˚ with 15˚ intervals under the conditions of $10^3 \leq Ra \leq 10^7$. It is found out that stronger vortexes occurred when heated wall moved from top to bottom wall. Subhani [9] researched the natural convection in a square enclosure with a hot cylinder in the center of the enclosure and cold winglets around it. Winglets increased vorticity in the enclosure and caused higher heat transfer. The best enhancement in heat transfer has been obtained with the winglets at 45˚ degrees. Sheikholeslami and Shamlooei [10] carried out a study to understand behaviour of $Fe_3O_4$/water nanofluid under natural convection with thermal radiation. Uniform and constant heat flux has been applied to inner wall. The working range of this study is $10^3 \leq Ra \leq 10^5$. Control volume based finite element method has been utilized to perform a study. It is concluded that the usage of thermal radiation has weaker effect in natural convection by using $Fe_3O_4$/water nanofluid. Dogonchi and Hashim [11] studied a wavy circular shape enclosure under natural convection to determine the effect of several parameters such as Rayleigh number ($10^3 \leq Ra \leq 10^5$), radiation parameter ($0 \leq Rd \leq 0.3$), the shape factor of nanoparticles ($m$=3, 4.8, 5.7), the volumetric concentration of $Fe_3O_4$/water (2%, 4%). It is determined that the usage of a higher volumetric concentration with a higher Rayleigh number presents a higher convective heat transfer rate. Sheikholeslami et al. [12] performed natural convection with Coulomb forces to detect the effect of Coulomb force in existence of thermal radiation by using $Fe_3O_4$/water nanofluid. Likewise, other researchers mentioned, in this study determined that the presence of thermal radiation has weaker effect on convective heat transfer rate under natural convection [10,11]. Moraveji and Hejazian [13] carried out an investigation heat transfer effect of $Fe_3O_4$/water nanofluid in rectangular cavity under natural convection. To determine the heat transfer effect, the range of Rayleigh number and volumetric concentration of nanoparticles has been applied as $10^3 \leq Ra \leq 10^5$, $0 \leq \varphi \leq 14\%$, respectively. While the magnitude of Rayleigh number presents positive effect in heat transfer rate, addition of nanoparticles to base fluid establishes a negative effect for this study.

Even though natural convection in a square enclosure has been widely investigated in the literature, using nanofluid as working fluid has not been studied detailly and more data presented in this manuscript is going to provide detailed insight on the heat transfer enhancement mechanisms in the enclosure to the literature.

# 2. Material and Method

## 2.1. Problem Description and Mathematical Formulas

In this study, a 2D enclosure has been designed to investigate the buoyancy effect of $Fe_3O_4$/water under natural convection. The dimensions and boundary conditions of the calculation domain can be seen in Fig. 1. As can be seen in Fig. 1, while the left wall *($T_H$)* is kept at higher temperature condition, which is changing with Grashof *(Gr)* number, the right wall is also kept at constant lower temperature condition ($T_L$=298 *K*). Also, the top and bottom walls are in an insulated wall condition, which leads to an impermeable situation. The working fluid has been considered Newtonian and incompressible. The nanoparticle has been taken in uniform sizes and well dispersed in the base fluid. So, it is noted that the nanofluid and water have been assumed at the same velocity and in thermal equilibrium. Since the nanoparticle dispersion in base water disperses homogeneously, the computational domain has been modelled using the single-phase approach [14]. Also, the thermophysical properties of both water and $Fe_3O_4$/water nanofluid have been taken as constant, and the thermal expansion coefficient has been modelled with Boussinesq approximation.

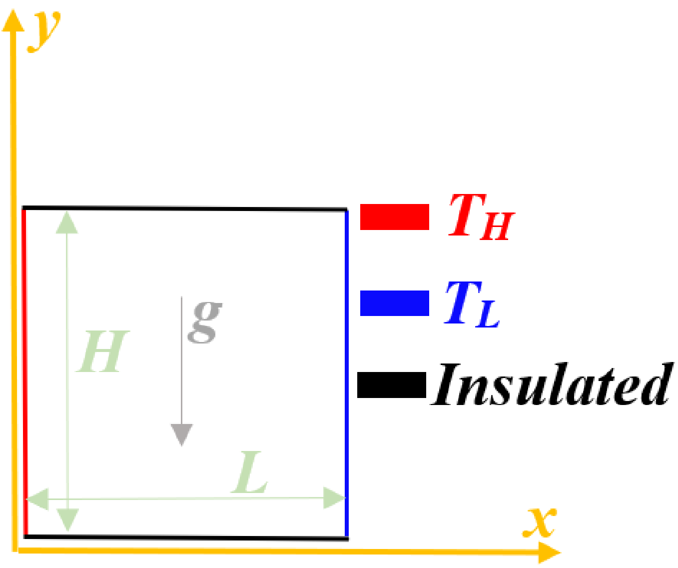


**Fig. 1.** Schematic of study

Regarding these phenomena, the boundary and initial conditions have been adjusted as below:

$$u = 0, v = 0, T = 0 \quad @ \quad 0 \leq x \leq L,\ \ 0 \leq y \leq H,\ \ t = 0$$

$$u = 0, v = 0, \frac{\partial T}{\partial y} = 0 \quad @ \quad 0 \leq x \leq L,\ \ y = 0 \ and \ y = H,\ \ 0 \leq t \leq \tau$$

$$u = 0, v = 0, T = T_H \quad @ \quad x = 0,\ \ 0 \leq y \leq H,\ \ 0 \leq t \leq \tau$$

$$u = 0, v = 0, T = T_L \quad @ \quad x = L,\ \ 0 \leq y \leq H,\ \ 0 \leq t \leq \tau$$

By using these boundary conditions above-mentioned, the governing equations have been calculated in dimensional form as following:

Continuity equation:

$$\frac{\partial u}{\partial x}+\frac{\partial v}{\partial y}=0 \tag{1}$$

Momentum equation:

$$u\frac{\partial u}{\partial x}+v\frac{\partial u}{\partial y}=-\frac{1}{\rho_{nf}}x\frac{\partial P}{\partial x}+\nu_{nf}\left(\frac{\partial^2 u}{\partial x^2}+\frac{\partial^2 u}{\partial y^2}\right) \tag{2}$$

$$u\frac{\partial v}{\partial x}+v\frac{\partial v}{\partial y}=-\frac{1}{\rho_{nf}}x\frac{\partial P}{\partial v}+\nu_{nf}\left(\frac{\partial^2 v}{\partial x^2}+\frac{\partial^2 v}{\partial y^2}\right)+\beta_{nf}g\left(T-T_c\right) \tag{3}$$

Energy equation:

$$u\frac{\partial T}{\partial x}+v\frac{\partial T}{\partial y}=\alpha_{nf}\left(\frac{\partial^2 T}{\partial x^2}+\frac{\partial^2 T}{\partial y^2}\right) \tag{4}$$

Also, the nanofluid thermo-physical properties can be calculated as below. Also, thermo-physical properties of nanoparticle and base fluid are given in Table 1.

Density [15]:

$$\rho_{nf}=\varphi\rho_{np}+\left(1-\varphi\right)\rho_{bf} \tag{5}$$

Specific heat [16]:

$$C_{p,nf}=\frac{\varphi\left(\rho C_p\right)_{np}+\left(1-\varphi\right)\left(\rho C_p\right)_{bf}}{\rho_{nf}} \tag{6}$$

Viscosity [17]:

$$\mu_{nf}=\mu_{bf}\left(123\varphi^2+7.3\varphi+1\right) \tag{7}$$

Thermal conductivity [18]:

$$k_{nf}=k_{bf}\frac{\left(k_{np}+2k_{bf}\right)-2\varphi\left(k_{bf}-k_{np}\right)}{\left(k_{np}+2k_{bf}\right)+\varphi\left(k_{bf}-k_{np}\right)} \tag{8}$$

Thermal expansion coefficient [19]:

$$\left(\rho\beta\right)_{nf}=\left(1-\varphi\right)\left(\rho\beta\right)_{bf}+\varphi\left(\rho\beta\right)_{np} \tag{9}$$

Grashof number can be calculated as following [20]:

$$Gr=\frac{g\beta_f\Delta TH^3}{v_f^2} \tag{10}$$

where $\Delta T$ is the temperature difference between hot wall and cold wall. $H$ is the height of the enclosure. $v$ is kinematic viscosity.

**Table 1**. Thermophysical properties of medium [21].

| Property | Water | $Fe_3O_4$ |
|---|---|---|
| $C_p$ | 4179 | 670 |
| $\rho$ | 997.1 | 5200 |
| $k$ | 0.6 | 6 |
| $\beta$ | $2.1x10^{-4}$ | $1.3x10^{-5}$ |

Then, the local Nusselt and average Nusselt numbers can be calculated with Eq. (11) and Eq. (13).

$$Nu=\frac{Q}{Q_{cond,fluid}}=-\frac{\left(k_{eff}\right)_{stagnant}}{k_f}\frac{\partial\theta}{\partial X} \tag{11}$$

where,

$$Q=-\left(k_{eff}\right)_{stagnant}A\frac{\partial T}{\partial x} \tag{12}$$

$$\overline{Nu}=\int_0^L Nu(y)dy/L \tag{13}$$

## 2.2. Mesh study and Validation

The present study has been calculated by using ANSYS Fluent *v2020R2*. The computational study has been applied by using SIMPLE pressure-velocity coupling model with second-order upwind scheme. All convergency criteria have been reached $10^{-8}$ approximation value. Also, Least-Squares Gradient scheme has been utilized in spatial discretization for the gradient. The finite volume method *(FVM)* has been utilized for all computations. All these procedures have been carried out in both water and nanofluid steps.

Before starting analyses, the mesh study should be performed to obtain better results in the numerical study. Also, all mesh studies have been applied at highest *Gr* number. As can be seen in Table 2, in order to decide the optimum mesh structure, several mesh studies have been done. From the calculations, it is concluded that there is no significant difference between M4 and M5 in terms of average Nusselt number so M4 has been selected as the optimum mesh structure. The typical mesh structure is presented in Fig. 2.

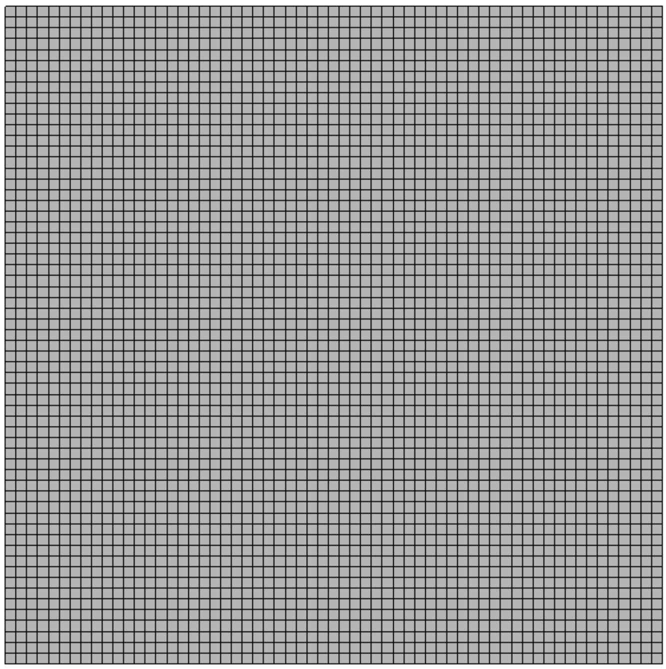

**Fig. 2**. Mesh structure for the enclosure.

**Table 2**. Mesh study for $Gr=10^5$

| Mesh No | Mesh | Avg. *Nu* (Present study) |
|---|---|---|
| **M1** | 11*x*11 | 6.158 |
| **M2** | 31*x*31 | 7.121 |
| **M3** | 41*x*41 | 7.982 |
| **M4** | 61*x*61 | 8.256 |
| **M5** | 71*x*71 | 8.467 |
| **M6** | 81*x*81 | 7.992 |

For the second step, the numerical domain should be validated with a study published in the literature in the same boundary conditions. For this purpose, numerical results have been validated with the data obtained from Khanafer et al. [20]. Comparison of streamlines between the present study and that of Khanafer et al. is given in Fig. 3. Also, numerical values have been compared Table 3. It is concluded from Table 3 that the maximum deviation between the present study and data of Khanafer et al. [20] is 8.06%, so the present computational domain is under acceptable conditions for further studies.

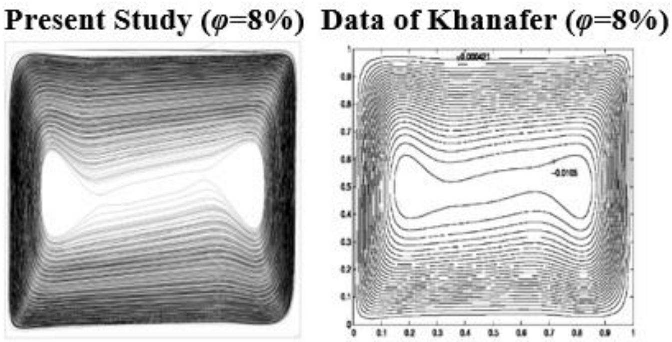


**Fig. 3.** Comparison of streamlines between the present study and that of Khanafer et al. [20] (φ=8% for Cu/water).

**Table 3**. Validation of present study with the literature [20].

| φ % | Present Study | | | Correlation of Khanafer et al. [20] | | | Deviation % | | |
|---|---|---|---|---|---|---|---|---|---|
| | *Gr*=$10^3$ | *Gr*=$10^4$ | *Gr*=$10^5$ | *Gr*=$10^3$ | *Gr*=$10^4$ | *Gr*=$10^5$ | Gr=$10^3$ | Gr=$10^4$ | Gr=$10^5$ |
| **0** | 1.9369 | 4.1047 | 8.256 | 1.9768 | 4.0574 | 8.3282 | 2.0573 | 1.1514 | 0.8746 |
| **4** | 2.09576 | 4.41359 | 8.8407 | 2.1141 | 4.3394 | 8.9070 | 0.8765 | 1.6804 | 0.7500 |
| **8** | 2.33518 | 4.87389 | 9.72715 | 2.2673 | 4.6539 | 9.5526 | 2.90 | 4.5129 | 1.7947 |
| **12** | 2.5779 | 5.33935 | 10.6309 | 2.4272 | 4.9820 | 10.226 | 5.84 | 6.6923 | 3.8087 |
| **16** | 2.80433 | 5.7725 | 11.4789 | 2.5915 | 5.3192 | 10.918 | 7.58 | 7.851 | 4.8848 |
| **20** | 3.0012 | 6.14829 | 12.2193 | 2.7592 | 5.6634 | 11.625 | 8.06 | 7.8861 | 4.8665 |

## 3. Results and Discussion

In this study, natural convection inside a square enclosure with a hot left wall, a cold right wall, and adiabatic top and bottom walls have been examined.

Table 4 depicts the average Nusselt number enhancements using $Fe_3O_4$/water nanofluid. Under natural convection condition, the effect of volumetric concentrations of nanofluid on heat transfer performance is weaker. 1.0% volumetric concentrations of nanofluid offers up to 0.74% enhancement, whereas enhancements of lower volumetric concentrations compared to distilled water are indistinctive. Enhancement obtained by using 1.0% volumetric concentrations of nanofluid in average Nusselt number takes place because of increment in thermal conductivity of working fluid. Also, higher *Gr* causes higher average Nusselt number for all cases.

Fig. 4 shows the local Nusselt number across the length of the hot wall using 1.0 vol.% $Fe_3O_4$/water nanofluid. The convection heat transfer rates are higher at lower portions of the hot wall. As the temperature of the fluid increases along the vertical length of the hot wall, the temperature gradient decreases and the heat transfer rate also diminishes. As *Gr* increases, the heat transfer rates increase.

Fig. 5 shows the local temperature across the axial length between the hot and cold walls using distilled water and $Fe_3O_4$/water nanofluids as a working fluid.

**Table 4.** Average Nusselt number variations for different Grashof numbers and nanoparticle volume fraction *(NPVF)* for present study ($Fe_3O_4$/water)

| φ (%) | *Gr*=$10^3$ | *Gr*=$10^4$ | *Gr*=$10^5$ | Enhancement (%) for *Gr*=$10^3$ | Enhancement (%) for *Gr*=$10^4$ | Enhancement (%) for *Gr*=$10^5$ |
|---|---|---|---|---|---|---|
| **0** | 1.9369 | 4.1047 | 8.256 | - | - | - |
| **0.01** | 1.93939 | 4.11302 | 8.26565 | 0.1286 | 0.2027 | 0.1169 |
| **0.1** | 1.93992 | 4.11391 | 8.26735 | 0.1560 | 0.2244 | 0.1375 |
| **1** | 1.95099 | 4.13506 | 8.30822 | 0.7275 | 0.7396 | 0.6325 |

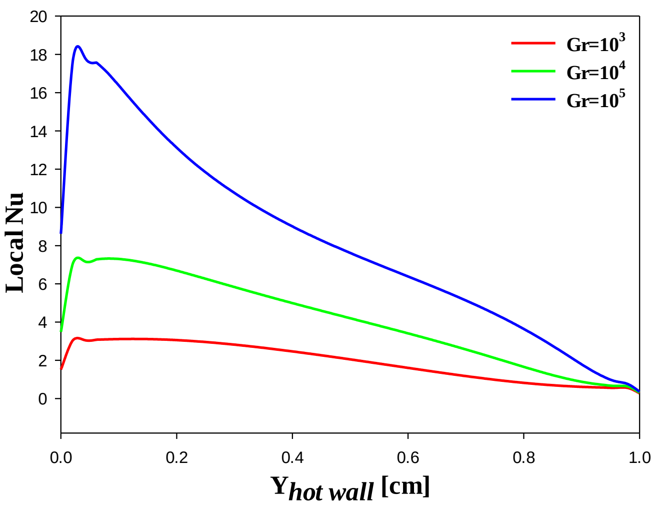


**Fig. 4.** Local Nusselt number distribution on the hot wall for φ=1%.

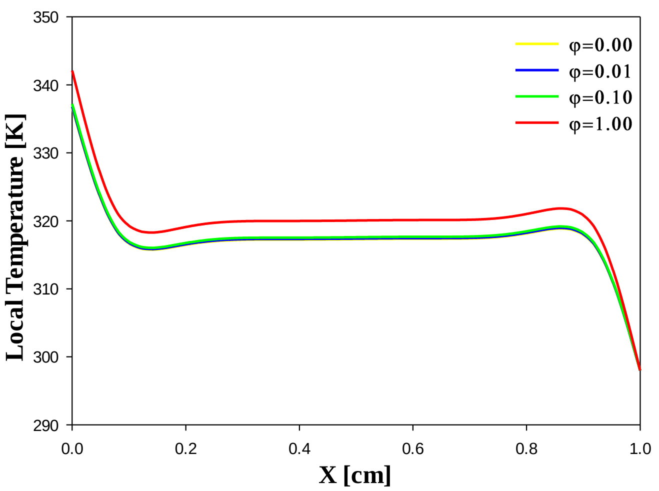


**Fig. 5.** Local temperature distribution along the axial length for *Gr*=$10^5$

As expected, nanofluid with higher volumetric concentrations offers higher temperature fluctuations. As the heat transfer occurs from the hot wall, temperatures at the axial lengths where it is closer to the hot wall are higher, whereas temperatures where it is closer to the cold wall are lower. Fig. 6 depicts the vertical velocity distribution along the axial length between the hot and cold walls. As the temperature gradient between the hot and cold walls increases, vertical velocity increases due to enhanced buoyancy-driven forces with higher *Gr*.

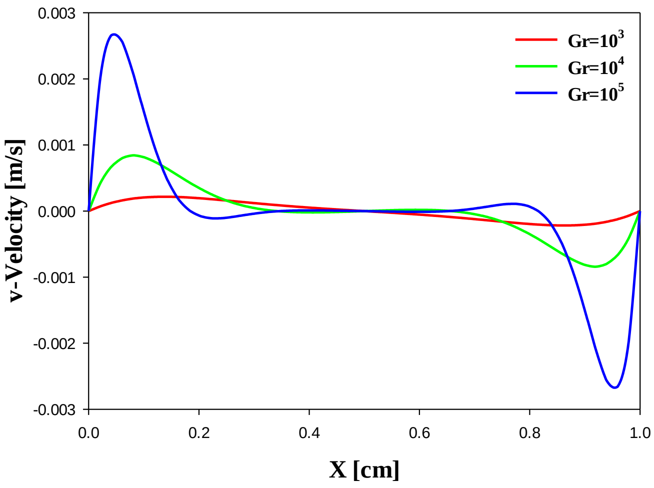


**Fig. 6.** Local v-Velocity distribution along the axial length for φ=1%.

Fig. 7 shows the temperature contours across the enclosure. Firstly, it is concluded that higher *Gr* contributes positively to the natural convection in the enclosure and higher volumetric concentrations are seen in a higher temperature gradient. Temperature contours of lower volumetric concentrations are similar as this situation. It shows why researchers study with higher volumetric concentrations of nanofluids in natural convection problems [13]. Fig. 8 represents the velocity contours across the enclosure. As the volumetric concentration of the nanofluid or *Gr* increase, velocity magnitudes increase because of higher buoyancy-driven forces. This mechanism is also reflected in vorticity contours illustrated in Fig. 9. Higher *Gr* and volumetric concentration of the nanofluid cause higher vorticity magnitudes.

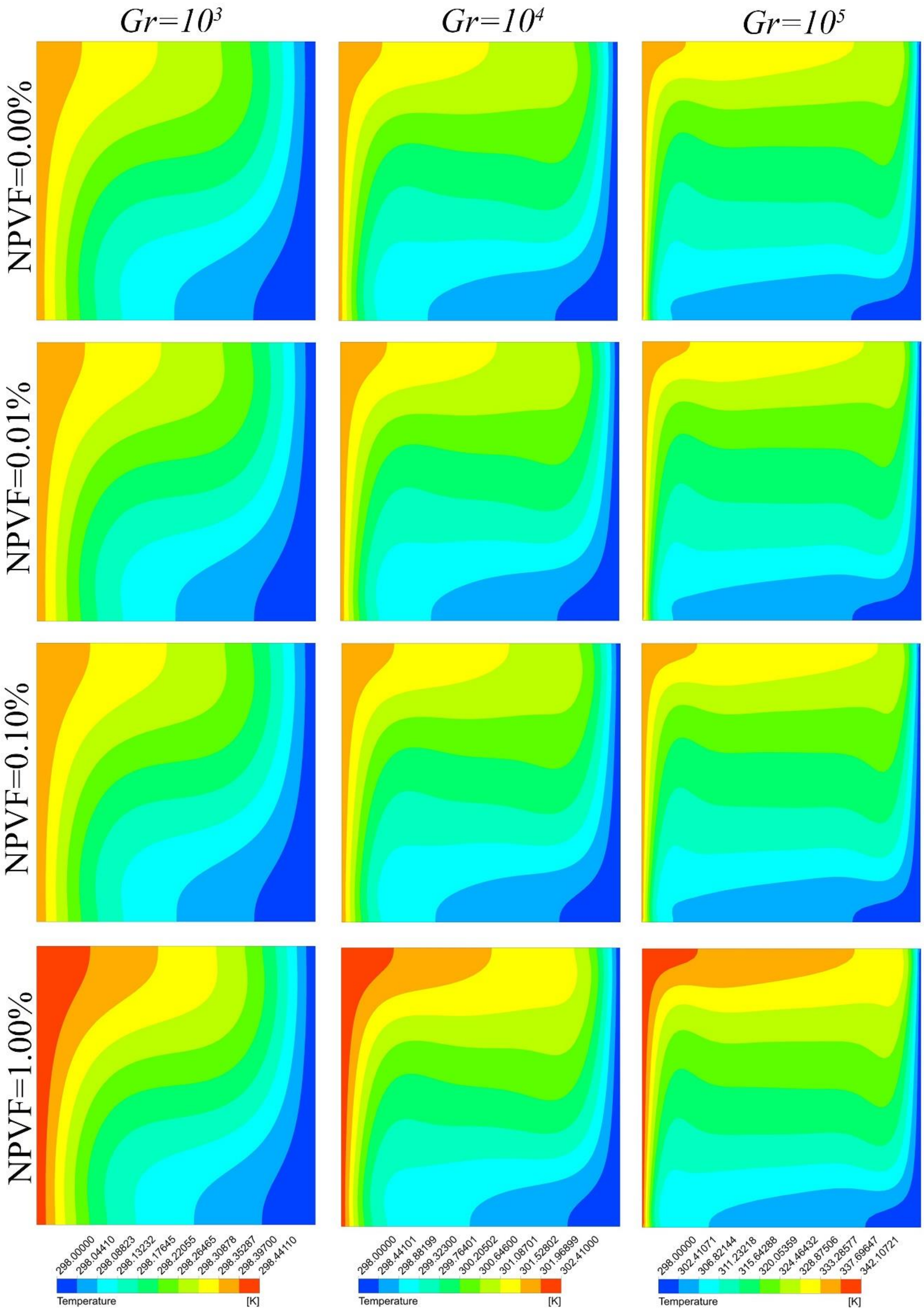


**Fig. 7**. Temperature contours for all cases.

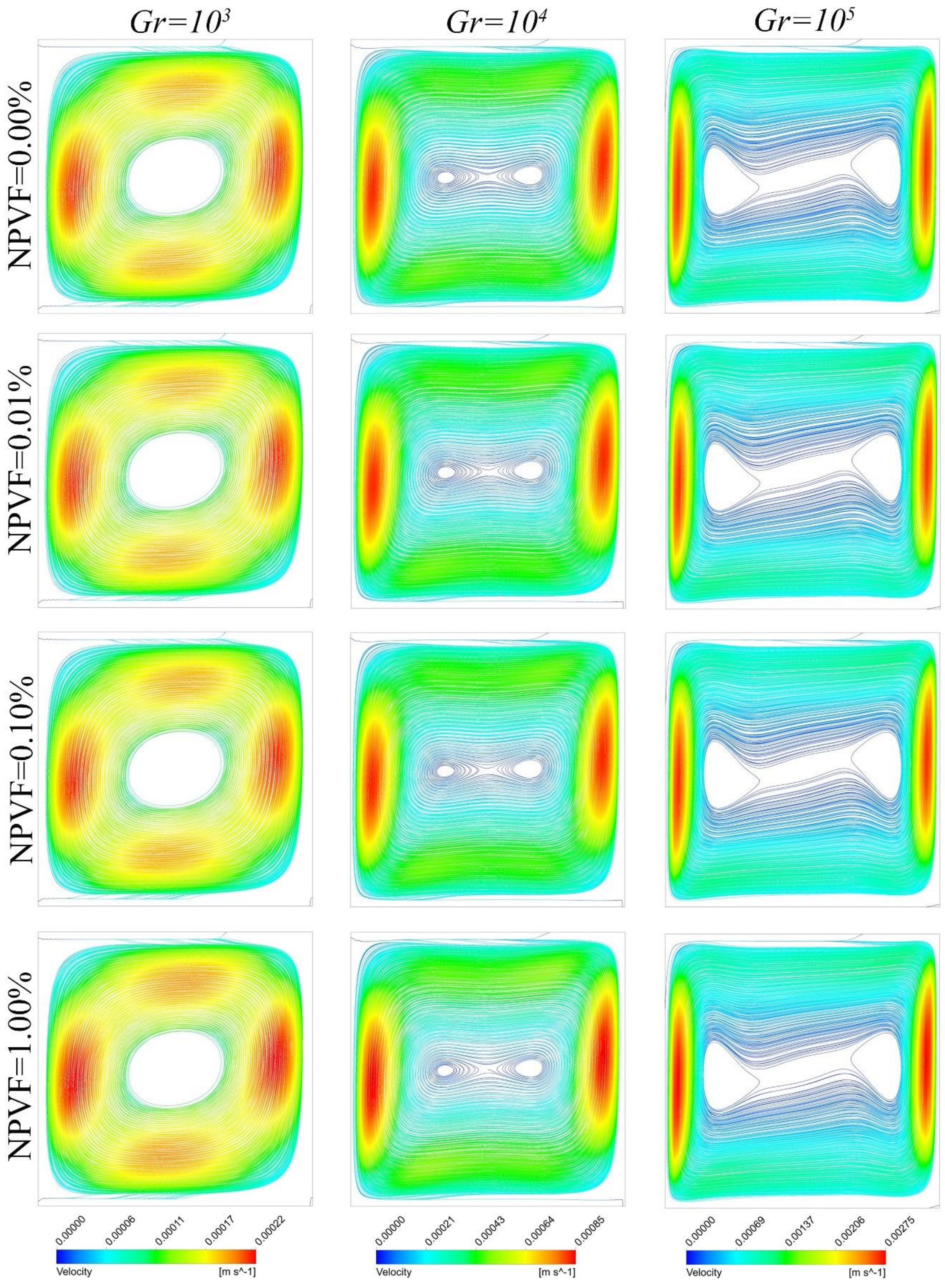


**Fig. 8**. Velocity streamlines for all cases.

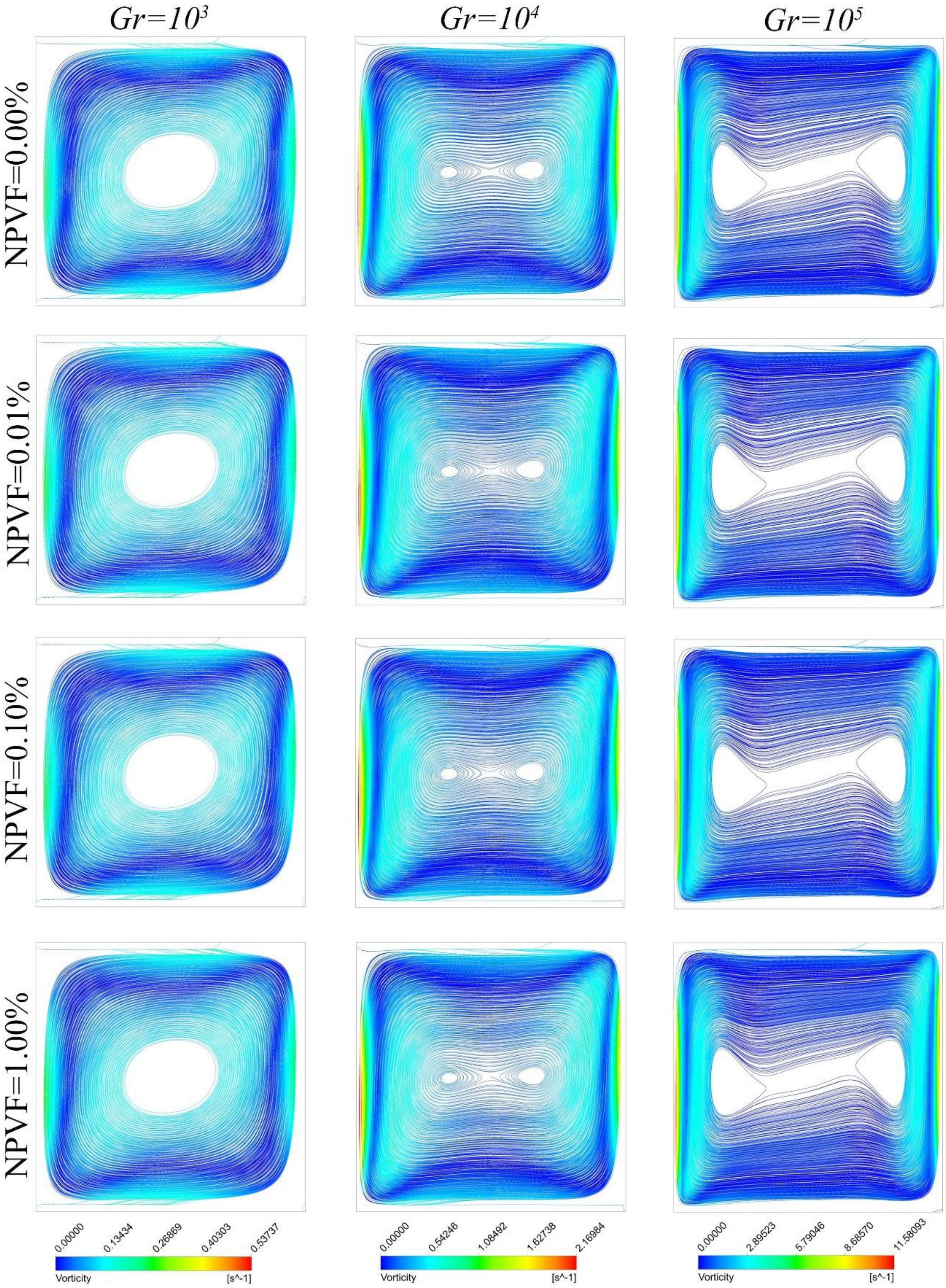


**Fig. 9**. Vorticity streamlines for all cases.

## 4. Conclusions and Recommendations

The natural convection heat transfer characteristics of nanofluid flow in a square enclosure have been examined under the conditions of $10^3 \leq Gr \leq 10^5$.

- Temperature distribution across the enclosure increaes with increasing volumetric concentrations of nanofluid.
- Higher *Gr* number and volumetric concentrations of nanofluid cause higher local Nusselt number, vertical velocity, and vorticity magnitudes.
- Higher heat transfer rates are obtained at the lower portions of the hot wall due to the greater temperature difference between the hot wall and the medium.
- As *Gr* number increases, flow structures develop in enclosure.

## References


[1] Savio, R. R., Shaik, S., & Kumar, R. S. (2021). Numerical study of natural convection around a square cylinder within a square enclosure for different orientations. Journal of Thermal Analysis and Calorimetry, 1-15.

[2] Singh, A. P., Kumar, A., & Singh, O. P. (2021). Natural convection solar air heater: Bell-mouth integrated converging channel for high flow applications. Building and Environment, 187, 107367.

[3] Pera, L., & Gebhart, B. (1973). Natural convection boundary layer flow over horizontal and slightly inclined surfaces. International Journal of Heat and Mass Transfer, 16(6), 1131-1146.

[4] Jones, H., & Marshall, J. (1993). Convection with rotation in a neutral ocean: A study of open-ocean deep convection. Journal of Physical Oceanography, 23(6), 1009-1039.

[5] Kim, B. S., Lee, D. S., Ha, M. Y., & Yoon, H. S. (2008). A numerical study of natural convection in a square enclosure with a circular cylinder at different vertical locations. International journal of heat and mass transfer, 51(7-8), 1888-1906.

[6] Bhattacharya, M., & Basak, T. (2021). Analysis of multiple steady states for natural convection of Newtonian fluids in a square enclosure. Physics of Fluids, 33(10), 103605.

[7] Hadidi, N., Rebhi, R., Bennacer, R., Menni, Y., Ameur, H., Lorenzini, G., ... & Ahmad, H. (2021). Thermosolutal natural convection across an inclined square enclosure partially filled with a porous medium. Results in Physics, 21, 103821.

[8] Liang, X., Zhang, H., & Tian, Z. (2021). A fourth-order compact difference algorithm for numerical solution of natural convection in an inclined square enclosure. Numerical Heat Transfer, Part A: Applications, 80(6), 255-290.

[9] Subhani, S. (2021). Natural Convection Heat Transfer Enhancement of Circular Obstacle within Square Enclosure. Journal of Thermal Analysis and Calorimetry, 1-19.

[10] Sheikholeslami, M., & Shamlooei, M. (2017). Fe3O4–H2O nanofluid natural convection in presence of thermal radiation. International Journal of Hydrogen Energy, 42(9), 5708-5718.

[11] Dogonchi, A. S. (2019). Heat transfer by natural convection of Fe3O4-water nanofluid in an annulus between a wavy circular cylinder and a rhombus. International Journal of Heat and Mass Transfer, 130, 320-332.

[12] Sheikholeslami, M., Shehzad, S. A., & Kumar, R. (2018). Natural convection of Fe3O4-ethylene glycol nanouid under the impact of electric field in a porous enclosure. Communications in Theoretical Physics, 69(6), 667.

[13] Moraveji, M. K., & Hejazian, M. (2013). Natural convection in a rectangular enclosure containing an oval-shaped heat source and filled with Fe3O4/water nanofluid. International communications in heat and mass transfer, 44, 135-146.

[14] Gürdal, M., Pazarlıoğlu, H. K., Tekir, M., Arslan, K., & Gedik, E. (2021). Numerical Investigation on Turbulent Flow and Heat Transfer Characteristics of Ferro-Nanofluid Flowing in Dimpled Tube under Magnetic Field Effect. Applied Thermal Engineering, 117655.

[15] Pak, B. C., & Cho, Y. I. (1998). Hydrodynamic and heat transfer study of dispersed fluids with submicron metallic oxide particles. Experimental Heat Transfer an International Journal, 11(2), 151-170.

[16] Xuan, Y., & Roetzel, W. (2000). Conceptions for heat transfer correlation of nanofluids. International Journal of heat and Mass transfer, 43(19), 3701-3707.

[17] Wang, X., & Xu, X. S. U. S. ChoiS., 1999,". Thermal conductivity of nanoparticle-fluid mixture, 474-480.

[18] Hamilton, R. L., & Crosser, O. K. (1962). Thermal conductivity of heterogeneous two-component systems. Industrial & Engineering chemistry fundamentals, 1(3), 187-191.

[19] Alsabery, A. I., Gedik, E., Chamkha, A. J., & Hashim, I. (2020). Impacts of heated rotating inner cylinder and two-phase nanofluid model on entropy generation and mixed convection in a square cavity. Heat and Mass Transfer, 56(1), 321-338.

[20] Khanafer, K., Vafai, K., & Lightstone, M. (2003). Buoyancy-driven heat transfer enhancement in a two-dimensional enclosure utilizing nanofluids. International journal of heat and mass transfer, 46(19), 3639-3653.

[21] Ghaffarpasand, O. (2016). Numerical study of MHD natural convection inside a sinusoidally heated lid-driven cavity filled with Fe3O4-water nanofluid in the presence of Joule heating. Applied Mathematical Modelling, 40(21-22), 9165-9182.